DØ Note: 2807
December 1995

Status Report: Search for Top in the All-Jets Channel

S. Ahn, N. Amos, P. Bhat, C. Cretsinger, J. McDonald, J. Moromisato, H. Prosper, C. Stewart, E. Won, R. Yamada

The DØ All-Jets Group

Abstract

We report on recent developments in, and preliminary results for, the search for $t\bar{t}$ production in the all-jets channel. These developments include more data and improvements in our muon-tagging algorithms. We find a cross section for $t\bar{t}$ production of 4.4 ± 4.9 pb for the case where a single muon-tag is required, and 3.9 ± 9.8 pb for the case where two muon-tags are required in the data.

1 Introduction

According to the Standard Model, the top quark is produced at the Tevatron primarily in the form of $t\bar{t}$ pairs. Each top quark decays to a W boson and a b quark, and the subsequent decays of the two W bosons distinguish the different channels. The "all-jets" channel consists of events in which both W bosons decay into light quarks (observed as jets); such events usually contain six (or more) high-momentum jets. The Standard Model predicts that the branching fraction for $t\bar{t} \rightarrow$ all-jets is 44%, largest of any decay channel.

Identifying a clear signal from $t\bar{t} \rightarrow$ all-jets would add to the significance of the top-quark signal observed at DØ and confirm the predictions of the Standard Model for $t\bar{t}$ decay. However, the signal is obscured by an enormous background consisting of events from other QCD (and semi-weak) processes that produce six or more jets. The cross section for such processes is on the order of a thousand times as large as the $t\bar{t}$ cross section.

Previous efforts to identify a $t\bar{t}$ signal in the all-jets channel have been documented elsewhere [1, 2, 3, 4]. In those references, we described kinematic selection criteria that can discriminate between $t\bar{t}$ and background events. We have also shown that the identification of b-quark jets using the presence of low-p_T muons ("muon-tagging") improves the signal-to-background ratio by about a factor of five. Furthermore, provided that muon-tagging is not strongly dependent on kinematic requirements, it can be used to estimate the remaining background. Using these techniques, we have not yet seen a clear $t\bar{t} \rightarrow$ all-jets signal.

This note describes recent developments in the search for $t\bar{t} \rightarrow$ all-jets at DØ. In Section 2, we define the data samples used in our search. In Section 3, we review the existing tools for selection of candidate events in the all-jets channel, namely, kinematic parameters and muon-tagging. In Section 4, we describe and compare four possible methods of defining optimal kinematic selection criteria that can be used for improving the ratio of signal to background. In Section 5, we present updated results from an analysis using the random grid search to optimize selection criteria as as been done in the past [3, 4]. In Section 6, we present a new method for determining the $t\bar{t}$ cross section and the background tagging rate from a simultaneous fit of these quantities to the data. Section 7 lists some issues that require further study, and a summary is presented in Section 8.

2 Data Samples and Simulation of $t\bar{t}$ Signal

For this search, we use data corresponding to an integrated luminosity of 13 pb^{-1} from Run Ia and 80 pb^{-1} from Run Ib. (We do not reject events collected during the MRBS_LOSS and MICRO_BLANK intervals, when protons circulating in the Main Ring cause background spray in parts of the DØ detector.) Data from Run Ia were reconstructed using Version 11.19 of the DØRECO program [5]; data from Run Ib were reconstructed using Versions 12.13–12.19. The standard energy-scale corrections of Version 5.0 of the program CAFIX [6] have been applied.

In previous studies, we have defined jets using a cone algorithm with a radius ($\mathcal{R} = \sqrt{\Delta\eta^2 + \Delta\phi^2}$, where η denotes pseudorapidity, and ϕ the azimuthal angle) of 0.3. However, due to concerns about the out-of-cone showering corrections and the sensitivity of muon-tagging in this algorithm, we have now chosen to use an $\mathcal{R} = 0.5$ cone to define jets in the offline analysis. (The $\mathcal{R} = 0.3$ cone algorithm is still used at Level 2 of the trigger.)

We select a "generic" data sample consisting of events that have at least five jets, where the $\mathcal{R} = 0.5$ cone algorithm is used to define jets. The search for a signal is concentrated on a subset of this sample (the "search" sample), which contains only events with at least six jets (again, defined using the $\mathcal{R} = 0.5$ cone algorithm). We also reject events that are considered in the lepton+jets and dilepton channels by requiring that our events not have any isolated electrons or muons with large p_T. The criteria used to select these samples were discussed in detail in Refs. [1, 3, 4], and are summarized in Table 1.

As was done in our previous studies, we use the presence of a low-p_T muon to tag b-quark jets. The requirements used to identify these muon-tags are the same as those used in the lepton+jets+μ-tag channels [8]:

- For Run Ia and for the latter part of Run Ib (run numbers after 89000), a fully reconstructed muon track is required to be present in the central (CF) or forward (EF) region of the WAMUS chambers ($|\eta| < 1.7$). Tracks that include hits in the SAMUS chambers are rejected. For the first part of Run Ib (run numbers 70000–89000) tracks are restricted to the CF region ($|\eta| < 1$).

- An acceptable track must satisfy the high-quality muon requirements. These include the quality (χ^2 of the fit) of the track in both the bend and non-bend views, the projection of the inner track segment to the vertex, and the number of chambers along the track that have a hit. (The quality word IFW4=0 is required for muons in the EF region; IFW4=1 or 0 is allowed for muons in the CF region.)

Generic Data Sample			
Requirement		observed cross section (nb)	efficiency for m_t=200
Level 1 trigger JET_MULTI [a]	Three large tiles $E_T > 15$ GeV	$0.4 \pm .1 \mu$b	1.00
Level 2 filter JET_MULTI [a]	Five $\mathcal{R}$=0.3 L2 jets $\|\eta\| < 2.5$, $E_T > 10$ GeV	20 ± 5 nb	0.93
Five jets	DØRECO, $\mathcal{R}$=0.5 cone $\|\eta\| < 2.5$, $E_T > 10$ GeV	20 ± 5 nb	0.92
Bad data	BAD_RUN.RCP [b]	-	-
Cleanup	See Ref. [1]	-	-
H_T> 115 GeV	DØRECO R=0.5 jets	6.5 ± 0.5 nb	0.92
Search Data Sample			
No isolated [c] e or μ	${E_T}^e < 20$ GeV ${p_T}^\mu < 15$ GeV/c	6.5 ± 0.5 nb	0.92
Six jets	E_T> 10 GeV CAFIX (V4.2) $\|\eta\| < 2$	2 ± 0.5 nb	0.70
H_T>150 GeV	jet $\|\eta\| < 2.0$, $E_T > 15$ GeV	1.5 ± 0.3 nb	0.70

Table 1: Initial data selection criteria, used to define "generic" and "search" data samples.

Notes: [a] Level 1 trigger requirements varied over the period of Run Ia and Run Ib, but the efficiency for m_t=160 GeV/c^2 remained in the 95–98% range. A requirement that $H_T > 110$ GeV was added in Level 2 during Run Ib (after trigger list V10.2). [b] This is a list of runs where known hardware problems were likely to affect the quality of data; the list we use is kept on the FNALDØ analysis cluster in the directory TOP_DOC$HROOT:[GENERAL_INFO.RUN_1B]. [c] Isolation is defined using standard definitions from other top analyses [7].

- The calorimeter response in the track road must be consistent with the passage of at least one minimum ionizing particle. Specifically, we require that the energy deposited in the calorimeter towers in a 2×2 road in η-ϕ around the muon trajectory be at least 1.5 times the energy expected for a minimum ionizing particle. (Because these muons are expected to be inside jets, this requirement is very efficient for signal.) For data from Run Ib, we also require that some energy above threshold be present in at least one of the electromagnetic and three of the hadronic layers of the calorimeter.

- The muon p_T must exceed 4 GeV/c. This requirement reduces the contamination from π and K decays and favors decays from heavy quarks.

- A jet must be reconstructed (using the $\mathcal{R} = 0.5$ cone algorithm) within $\Delta\mathcal{R} = 0.5$ of the muon. This requirement enhances selection of muons that are products of semi-leptonic decays of heavy quarks.

At present, we do not have a reliable Monte Carlo simulation of the QCD multijet background. We therefore use data to model the background, as we have done previously [3]. In this analysis, all of the data from Run Ia are used to model the background, and the search for signal is restricted to data from Run Ib. The sacrifice of a large portion of the data sample, containing 14% of the available luminosity (including top candidates), ensures that the selection criteria are derived from an event sample that is statistically independent of the sample used in the actual search.

We continue to use the ISAJET Monte Carlo program to model the $t\bar{t}$ signal, and the generated event samples are described in Ref. [4].

3 Techniques for Event Selection

3.1 Kinematic Parameters

To distinguish signal from background, we use kinematic parameters based on the number of jets and the energies of the jets in an event. The parameters are calculated using jets[1] with $E_T > 10$ GeV (after CAFIX corrections) and $|\eta| < 2$. The four kinematic parameters are the usual:

- H_T^{3j}, which is the scalar sum of the E_T values of the jets, excluding the leading two.
- Aplanarity ($\mathcal{A}$), which is 3/2 of the smallest eigenvalue of the jet-momentum tensor.
- Centrality (C), which is the ratio of the sums of transverse and total energies of all the jets.
- Average jet count (N_{jets}^{A}), which is the number of jets weighted by and averaged over a range of E_T thresholds.

These parameters have been described in detail elsewhere [1, 3, 4]. Their distributions for data and for signal (modeled for m_t = 200 GeV/c^2) are shown in Fig. 1. While other parameters can also be useful, we find that this simple set is sufficiently effective in discriminating between $t\bar{t}$ signal and background. Methods of optimizing selection criteria based on these parameters will be discussed in Section 4.

3.2 Muon-Tagging

After the application of kinematic requirements, events are required to have a muon-tag (defined in Section 2). Such muons are characteristic of decays of heavy (b or c) quarks. Because nearly every $t\bar{t}$ event contains two high-E_T b-quark jets, while most background events should not, we expect that the muon-tagging rate will be higher for signal than for background. Indeed, Monte Carlo studies of $t\bar{t} \rightarrow$ all-jets events indicate that a muon-tag should be detected in about 20% of such events, while only about 3% of background events (*i.e.*, data) produce a muon-tag [3, 4].

The muon-tagging rate depends on the relative likelihood that a given jet is due to a b (or c) quark, the branching ratio of $b \rightarrow \mu + X$ and on the muon-detection efficiency. To first order, it should be independent of kinematic criteria. We can therefore use the observed muon-tagging rate in QCD jet

[1] Due to an error that was discovered late in the editing of this note, kinematic parameters were calculated using jets reconstructed with the $\mathcal{R} = 0.3$ cone algorithm. As indicated elsewhere, muon-tagging does use the $\mathcal{R} = 0.5$ cone algorithm.

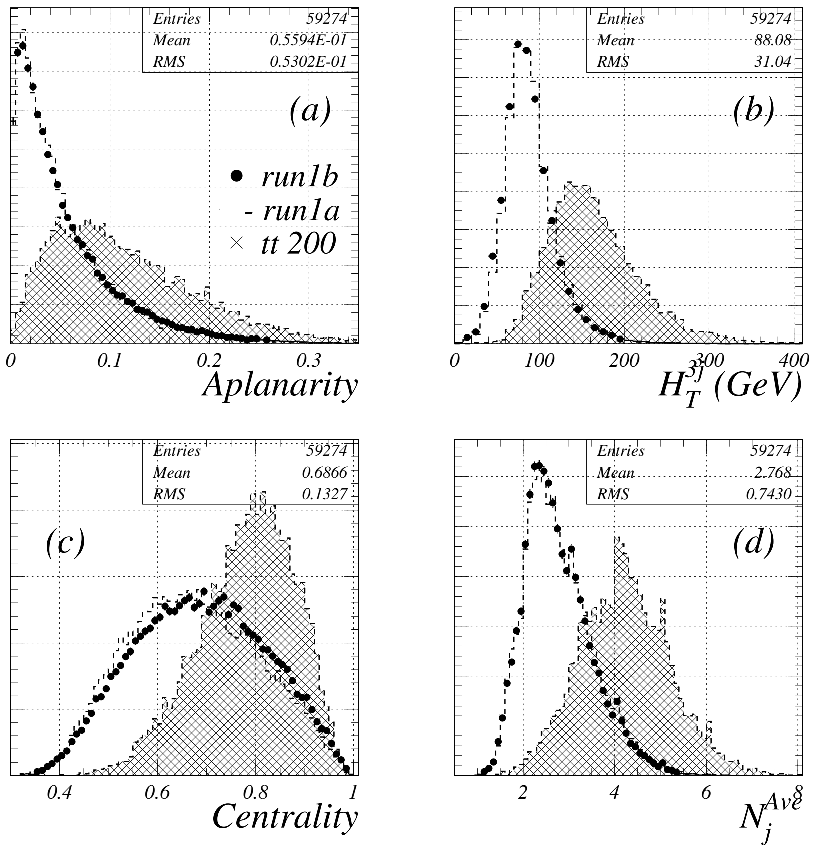

Figure 1: Distributions in kinematic parameters: aplanarity (a), H_T^{3j} (b), centrality (c), and average jet count N_{jets}^A (d) are shown for data from Run Ib (circles), Run Ia (dashed line), and ISAJET $t\bar{t}$ Monte Carlo for m_t = 200 GeV/c^2 (shaded). All distributions have been normalized to the same area.

production to estimate the number of background events to be expected in any data sample. As described elsewhere [3, 4], we have parametrized the muon-tagging rate per event for the generic (five or more jets) data sample, which is dominated by background from QCD jet production. We then used the parametrization to determine the expected background in our final data sample. Here, we extend our earlier work and describe a new approach for determining the muon-tagging rate for background.

3.2.1 Standard Estimate of Background

To model changes in the efficiency of the muon tracking chambers that occurred over the running period, we divided the data sample into three parts. Data from Run Ia comprise the first part. Data from Run Ib are divided into two periods, one prior to the cleaning of muon chambers in February 1995,[2] and one after the cleaning.[3]

If we consider only muons tracked in the CF chambers ($|\eta| < 1$) and jets with $|\eta| < 1$, we find that the tagging rate for each part of the data can be represented by a function of the form:

$$P_{\mu-\mathrm{tag}} = A + B \log E_T \tag{1}$$

This kind of parametrization has been used successfully in the past [3, 4], and the only change here is the use of jets that were reconstructed with the $\mathcal{R} = 0.5$ cone algorithm. Results for the three parts of the data sample are shown in Fig. 2.

With higher statistics, we have found that the probability that any generic jet is tagged depends not only on the E_T of that jet, but also on its η. Figure 3 shows the distribution in η of tagged jets in the generic sample, compared to the prediction from Eq. 1, which ignores any explicit dependence on η. The figure indicates that in fact, the tagging rate does depend on η, and that Eq. 1 is not an adequate model. Figure 4 shows the distribution in η for jets in the generic data sample and for jets in a "candidate" sample that was selected using typical kinematic criteria without requiring a muon-tag. The two distributions are not strongly different, which suggests that the effect of the η-dependence on a background estimate obtained considering only the E_T-dependence of the tagging rate is likely to be small. One can therefore

[2] Run numbers in the range 70000–89000.

[3] Run numbers after 89000.

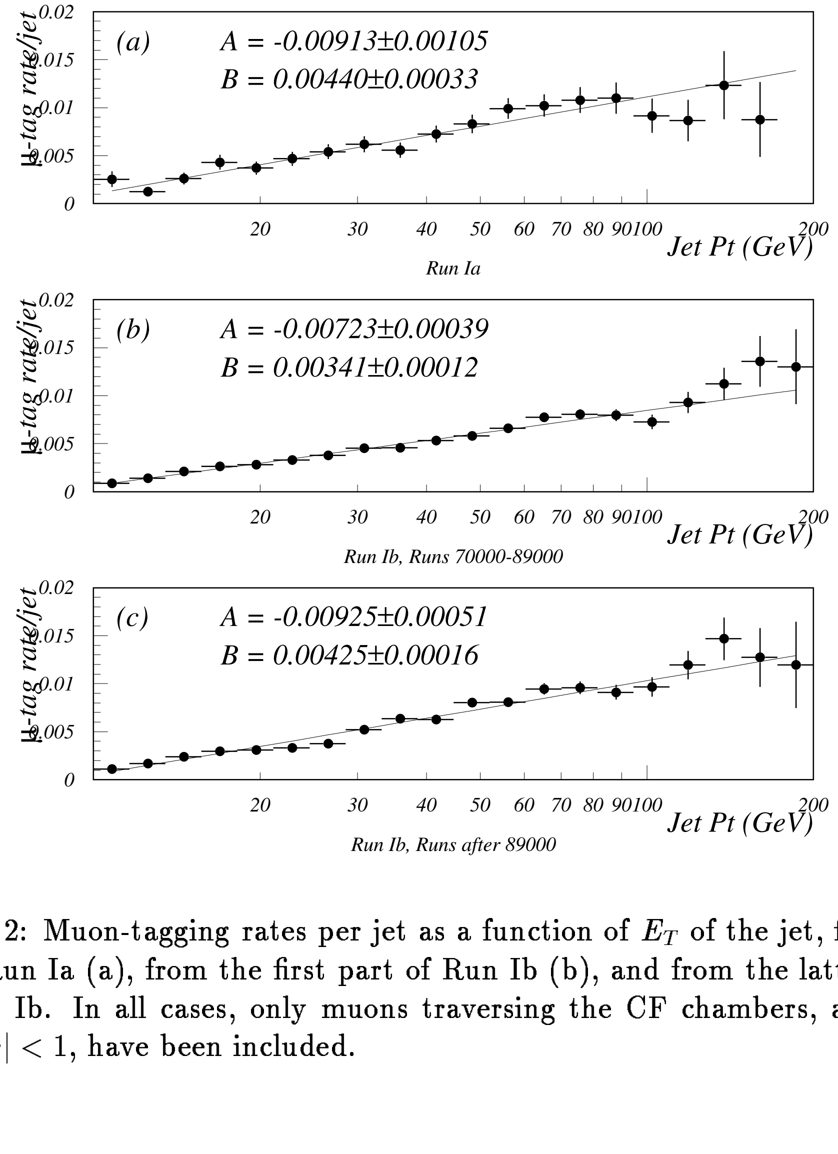

Figure 2: Muon-tagging rates per jet as a function of E_T of the jet, for data from Run Ia (a), from the first part of Run Ib (b), and from the latter part of Run Ib. In all cases, only muons traversing the CF chambers, and jets with $|\eta| < 1$, have been included.

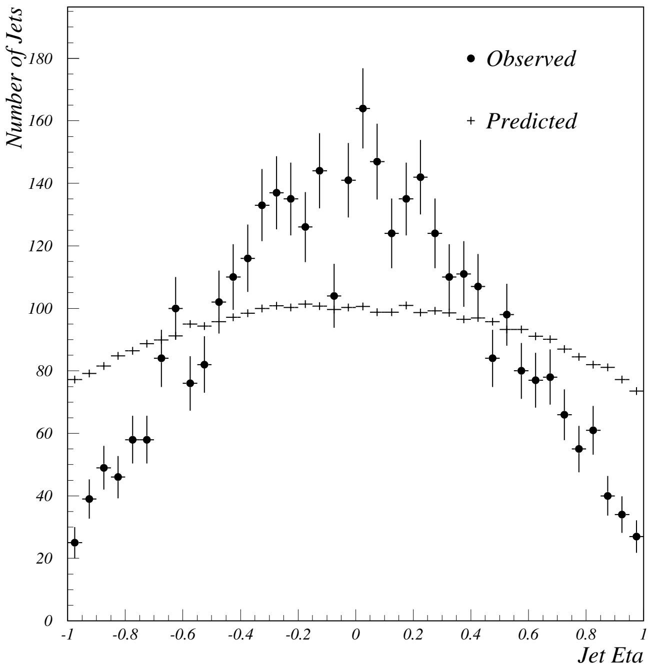

Figure 3: Distribution in η of tagged jets. The predicted (+) and observed ($\bullet$) distributions are seen not to be in good agreement.

choose to ignore this shortcoming of Eq. 1. However, it is clear that a more accurate model of muon-tagging of background events would be valuable.

3.2.2 Further Studies of Muon-Tagging

As a first step toward attaining a more accurate model of the tagging rate for jets, we have attempted to parametrize the muon-tagging rate for background as a function of both E_T and η. In constructing such models, we use the measured muon-chamber "efficiencies" shown in Figure 5. These plots represent the ratio of observed tags to expected tags as a function of η, where the most central muons ($|\eta| < 0.3$) have been used to normalize the tagging rate. (This is why the "efficiency" at times exceeds 1.) We found that these parametrizations appear to offer little advantage over the η-independent form

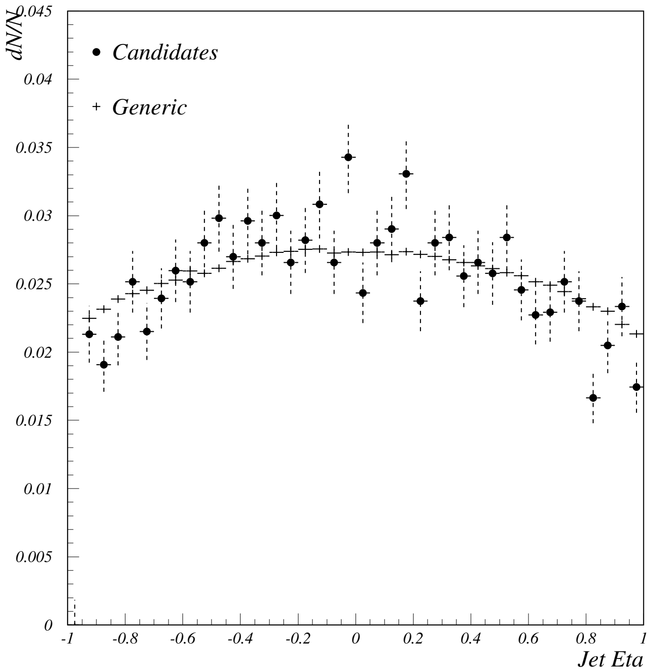

Figure 4: Distribution in η of jets in generic (+) and candidate ($\bullet$) data samples. A muon-tag has not been required. Both distributions have been normalized to the same area.

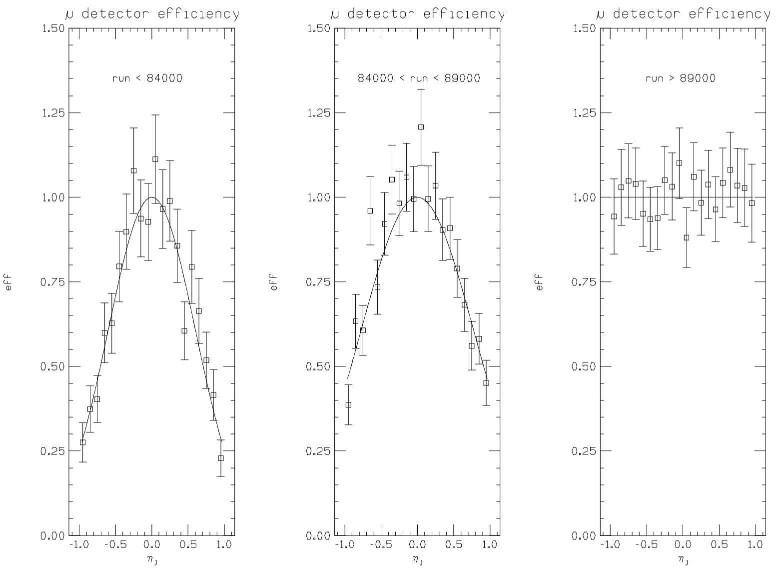

Figure 5: Muon-chamber "efficiency" as a function of jet η and run number.

of Eq. 1, and we have concluded that modeling the tagging rate as a function of E_T or other jet parameters appears to have general shortcomings.

We see evidence of some of the difficulty in Figure 6, where we examine data events selected with six different sets of kinematic criteria, numbered 1–6, with higher numbers corresponding to more restrictive criteria. Part (a) shows the mean E_T of all jets in the events that satisfied each set of criteria. We see that the mean value of E_T increases as the criteria become more restrictive. Fig. 6(b) shows the calculated muon-tagging rate per event corresponding to each set of criteria. This tagging rate was based on a parametrization that depends on E_T and η of each jet. As one would expect, the calculated tagging rate increases with increasing mean E_T. However, the measured tagging rate, shown in Fig. 6(d), does not appear to increase as much as predicted. Fig. 6(c) shows that the mean E_T of the leading jet also does not appear to increase as the criteria are made more restrictive. This suggests that the tagging rate depends more on the leading jet than on other jets.

Nearly all the tagged jets are among the three jets with largest E_T in an event. For this reason, we have considered the possibility that the tagging rate can be modeled more accurately by a function of E_T of the leading jet

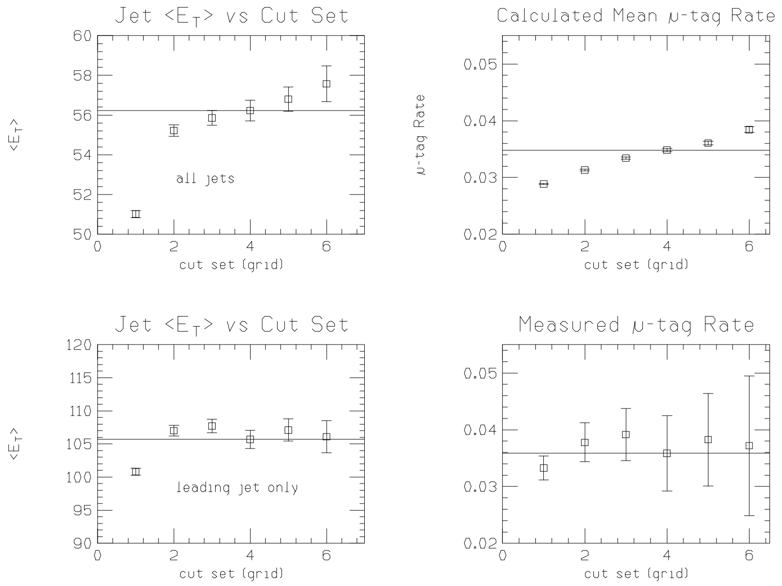

Figure 6: Properties of data samples that satisfy six sets of kinematic criteria. For each set of criteria, we show: in (a), the mean E_T of jets in the events that satisfied the kinematic criteria; in (b), the calculated tagging rate per event (using a function of jet E_T and η); in (c), the mean E_T of the leading jet; and in (d), the measured tagging rate.

(or perhaps H_T), rather than E_T of each jet, but no reliable models of this kind have yet been constructed [9]. We have therefore turned to a different approach to estimating the muon-tagging rate for background events.

We hypothesize that the fraction of QCD events that contain heavy quarks may be related to the "temperature" of the event, *i.e.*, to the hardness of the scatter. In the absence of a model that accurately predicts the tagging rate in the region where signal may dominate, we shall assume that in this region, the temperature of a typical QCD event is high enough that there is flavor-blindness. That is, the fraction of background events that include a heavy quark does not depend on the selected kinematic criteria. In other words, the tagging rate per background event, ϵ, is a constant in the region of phase space where signal is strong. This assumption will be employed in Section 6.

The lack of correlation between the p_T of the muon and the E_T of the tagged jet appears to be consistent with the above assumption. For tagged

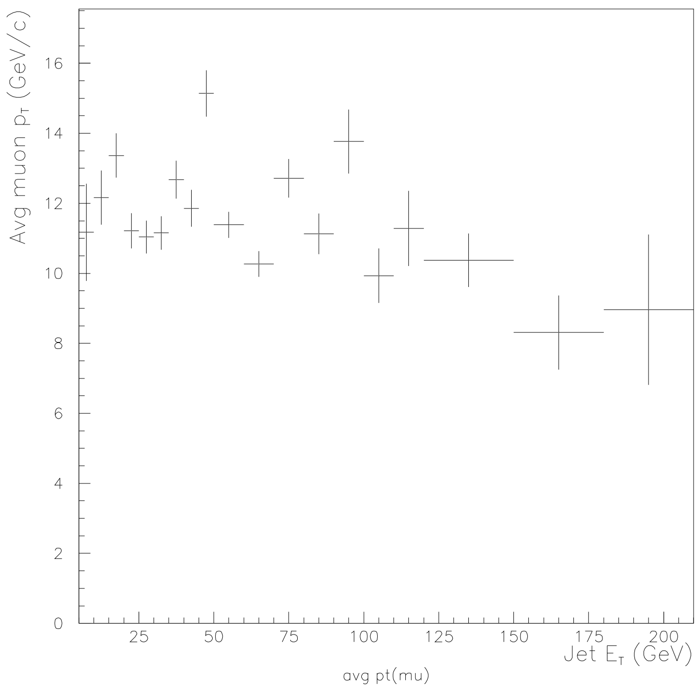

Figure 7: Mean muon p_T as a function of E_T of the tagged jet, for the generic data sample. No strong correlation is evident.

jets in the generic data sample, we have found that the average muon p_T is nearly independent of jet E_T, for $E_T < 100$ GeV. This can be seen in Fig. 7. This implies that the E_T of the tagged jet is a poor measure of the boost of the original hadron that decayed semi-leptonically. Thus, the probability that a muon from heavy-quark decay passes our $p_T \geq 4$ GeV/c cutoff does not depend on E_T of the tagged jet. Given our assumption of flavor-blindness, this is a necessary condition for the tagging rate per background event to be a constant.

If the data include a contribution from $t\bar{t} \rightarrow$ all-jets, then the measured tagging rate should increase as more restrictive kinematic criteria are used to improve the signal-to-background ratio. To illustrate this effect, we have used ISAJET Monte Carlo to model $t\bar{t}$ production, assuming a cross section of 8.3 pb, and we have modeled the background by subtracting the predicted $t\bar{t}$

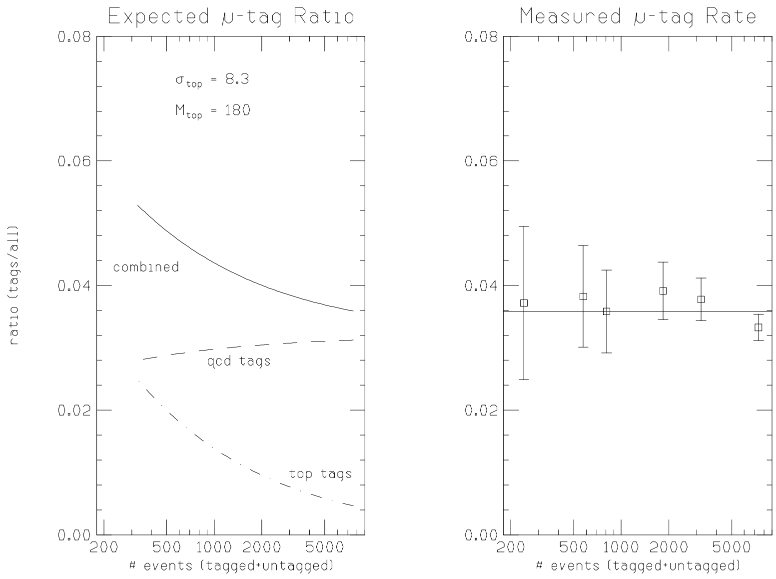

Figure 8: (a) Expected tagging rate (solid line) per event for a combination of $t\bar{t}$ and background, plotted as a function of the total number of events surviving kinematic criteria. The background was modeled by subtracting the expected $t\bar{t}$ contribution from DØ data. (b) Measured tagging rate per event, for six sets of kinematic criteria, again as a function of the number of events that survive.

contribution from the DØ data. We assume that about 3% of all QCD events will be tagged, independent of kinematic criteria, and that about 20% of $t\bar{t}$ events will be tagged. Figure 8(a) shows the overall muon-tagging rate as a function of the number of events satisfying sets of kinematic criteria. The smooth curve is generated by interpolating between three sets of criteria. Figure 8(b) shows the observed tagging rate for our data, for six sets of kinematic criteria. We see that the results are consistent with a constant tagging rate, or with a small contribution from $t\bar{t}$ production. In Section 6, we will use the change in measured tagging rate as a function of kinematic criteria to extract the cross section for $t\bar{t}$ production from the all-jets data.

4 Optimization Methods: A Comparison

The enormity of background relative to signal in the all-jets channel has forced us to investigate sophisticated multivariate analysis methods in order to achieve maximum discrimination between signal and background. Four methods of determining optimal selection requirements for the all-jets channel have been investigated. These have utilized the four kinematic parameters—namely, $\mathcal{A}$, H_T^{3j}, $\mathcal{C}$, and N_{jets}^A—that provide good discrimination between signal and background. In principle, if we knew the exact probability distribution functions for both signal and background in these four variables, we could derive the best discriminating function between signal and background. However, constructing such functions is quite difficult; in practice, approximations are necessary.

The four techniques we have examined for selecting optimal criteria are:

Random Grid Search This method involves sampling with great efficiency many possible sets of threshold requirements on the kinematic parameters [1, 3, 4, 10]. This technique has recently been adopted in other top analyses at DØ.

H-Matrix Two H-matrices are considered, one describing resemblance to signal, the other, resemblance to background. A threshold requirement is defined by a contour of constant statistical significance in the χ_s^2-χ_b^2 plane.

Discriminating Variable Function (DVF) This method assigns a value in the range $0 \leq f_i \leq 1$ for each of the four kinematic parameters in an event, with $f_i = 1$ signifying the region where signal is concentrated. The functions f_i are optimized using an iterative search procedure. A selection is made by applying a threshold requirement on the product of the four f_i values [11].

Artificial Neural Network (NN) This is a very general multivariate analysis tool that, through repeated training cycles, identifies features that distinguish signal from background [12, 13].

Each of these optimization methods represents an approximation (to some degree) to the complete probability distribution functions for $t\bar{t}$ signal and background. Each method also incorporates information about the correlations among the kinematic variables.

In order to compare the performance of the four algorithms, we have defined standard samples of data (used as background) and Monte Carlo $t\bar{t}$ signal. Using these samples to "train" each algorithm, we have determined optimal criteria based on each of the four methods. Performance of each is evaluated on the basis of the best signal-to-background ratio achieved for any given level of background. Figure 9 illustrates the performance of all four of these methods. We have plotted the expected number of tagged signal and background events resulting from many possible criteria defined using the grid search, the H-Matrix, the DVF method, and the NN. The signal is modeled using ISAJET $t\bar{t}$ Monte Carlo, with $m_t = 180$ GeV/c^2 and $\sigma_{t\bar{t}} = 8.3$ pb. The background is predicted by extrapolating the data from Run Ia to the integrated luminosity from Run Ib and applying an average background tagging rate.

Figure 9 suggests that the performance of all four techniques is nearly identical, especially when they are applied in the region of adequate signal-to-background (fewer than 50 background events). The NN method appears to do about 10% better in the region where large background remains. It seems unlikely that a significant improvement in the signal-to-background ratio over that achievable using the grid search will be found using any of the other tools.

5 Results of the Grid Search

Previously, we used the grid-search technique in conjunction with the standard background estimate from muon-tagging (Section 3.2.1) to search for a signal [3, 4]. We have continued to use that technique, and here we present our latest results. In this study, a randomly-selected subset of data from all of Run I was used for the background model, and the results were determined using the remaining data, which correspond to an integrated luminosity of 76.8 pb^{-1}. We restricted muon-tags to the CF region and used the fits of Eq. 1 (no η dependence) to estimate the expected background.

Table 2 shows four different sets of threshold values, with the expected backgrounds, observed yields, $t\bar{t}$ efficiency and the resulting $t\bar{t}$ cross section. The uncertainty on the cross section is dominated by statistical contributions. Sources of uncertainty in the acceptance include statistical sources, a 5% uncertainty in the energy scale, a 5% uncertainty in the muon-tagging rate, and an uncertainty of 10% reflecting the ambiguities in the Monte Carlo

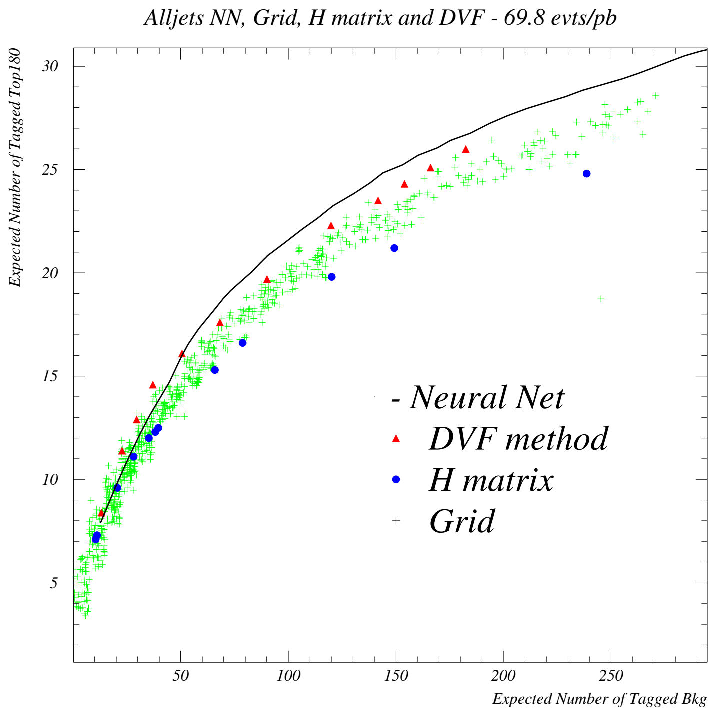

Figure 9: Comparison of Grid, H-Matrix, DVF, and Neural Network. For each algorithm, we show the expected yields for signal and background after muon-tagging, for a luminosity of 70 pb^{-1}. The background estimate is determined by extrapolating the data from Run Ia to the higher luminosity.

Thresholds				N_{bkg}	$N_{\mu-tag}$	$t\bar{t}$	Cross Section
$\mathcal{C}$	N^{A}_{jets}	$\mathcal{A}$	H_T^{3j} (GeV)	pred.	obs.	eff.	(pb)
0.702	3.94	0.157	183.9	3.01	4	0.0072	1.8 ± 3.7
0.706	4.58	0.124	167.5	5.70	7	0.0110	1.5 ± 3.2
0.542	4.01	0.082	145.4	32.8	43	0.0282	4.7 ± 3.9
0.601	3.92	0.059	144.6	44.4	57	0.0326	5.0 ± 4.1

Table 2: Threshold values, expected background and signal (m_t = 180 GeV/c^2), and cross section estimate for several sets of parameter thresholds.

model. Uncertainty in the background estimate includes a statistical contribution and the uncertainty in the fit to the background tagging rate, as well as a 10% uncertainty in the b-quark content of the background as a function of the kinematic parameters [4].

We define the cross section for $t\bar{t}$ production at the point where the expected statistical significance of signal is largest (the third point listed in Table 2). The result is: $\sigma_{t\bar{t}} = 4.7 \pm 3.9$ pb, assuming m_t =180 GeV/c^2. However, we caution that this result is still very preliminary because, as indicated in Section 3.2.2, we do not yet have an acceptable parametrization of the muon-tagging rate for the background.

6 Fitting Procedure to Determine $t\bar{t}$ Cross Section

Because the measured tagging rate per event is expected to be sensitive to the presence of $t\bar{t}$ in the data, as was illustrated in Fig. 8, we can employ the flavor-blindness assumption to extract both the $t\bar{t}$ cross section and the background tagging rate per event, ϵ, from a simultaneous fit of these constants to the data. Unlike the analysis of Section 5, this method does not rely on prior knowledge of the background tagging rate; instead, the value of ϵ is extracted from the observed tagging rate for events that satisfy several sets of kinematic criteria.

The advantage of determining $\sigma_{t\bar{t}}$ from such a fit, rather than from an

Set	Threshold Values				Acceptance	
No.	H_T^{3j} (GeV)	$\mathcal{C}$	$\mathcal{A}$	N_{jets}^A	$t\bar{t} \rightarrow$ all-jets	$\sum \varepsilon \times$ BR
1	137.7	0.543	0.048	3.39	0.371 ± 0.045	0.203 ± 0.024
2	141.7	0.551	0.052	3.73	0.339 ± 0.041	0.185 ± 0.022
3	142.1	0.596	0.054	3.88	0.321 ± 0.039	0.174 ± 0.021
4	147.8	0.596	0.059	3.99	0.289 ± 0.035	0.156 ± 0.019
5	156.0	0.613	0.060	4.38	0.226 ± 0.027	0.121 ± 0.015
6	176.3	0.668	0.075	4.75	0.135 ± 0.016	0.071 ± 0.009

Table 3: The six sets of threshold values used in the fit for cross section and tagging rate. The acceptances are determined prior to requiring a muon-tag.

excess of events that satisfy a particular set of kinematic requirements, is that all of the data are used, and therefore, all available information is incorporated into the determination of the $t\bar{t}$ cross section. In regions where there is a large contribution from $t\bar{t}$ production, the fit is sensitive to that cross section. In regions dominated by background, the fit extracts the background tagging rate, ϵ. The fit also provides the uncertainty in ϵ, and no further propagation of errors is required.

We define six independent event samples and perform a simultaneous χ^2 fit of the background tagging rate per event (ϵ) and the $t\bar{t}$ cross section ($\sigma_{t\bar{t}}$) to these samples. The samples are defined as follows. First, we choose six sets of thresholds on the usual kinematic parameters. Each set corresponds to a point on the optimal boundary from the grid search of Section 5. We require that the threshold values in successive sets do not decrease, and that the number of muon-tagged events passing the least restrictive thresholds be less than 150. The six sets of threshold values are listed in Table 3, along with the corresponding acceptances for $t\bar{t}$ events, determined using ISAJET Monte Carlo with $m_t = 180$ GeV/c^2. We then divide the data into six separate subsets (A_i), where A_1 contains events that passed the criteria of Set 1 but failed Set 2, and so on, up to A_6, which contains events that passed the criteria of Set 6. By construction, no event can appear in more than one of the A_i; the six samples are therefore statistically independent. Events in each of the A_i are divided into two categories: events with one muon-tag ("tagged") and all other events ("untagged").

The number of events (N_i) in A_i is the sum of background (N_i^{QCD}) and signal ($N_i^{t\bar{t}}$) contributions. For the tagged sample, we write:

$$N_i^{tagged} = N_i^{QCD} \epsilon e^{-\epsilon} + 0.2 N_i^{t\bar{t}}, \tag{2}$$

while for the untagged sample,

$$N_i^{untagged} = N_i^{QCD} (1 - \epsilon e^{-\epsilon}) + 0.8 N_i^{t\bar{t}}. \tag{3}$$

(We have assumed that the mean muon-tagging efficiency for $t\bar{t}$ events is 0.2, as obtained from Monte Carlo studies.) The total number of $t\bar{t}$ events (including tagged and untagged) can be expressed as:

$$N_i^{t\bar{t}} = \mathcal{L}\ \sigma_{t\bar{t}}\ \varepsilon, \tag{4}$$

where ε is the acceptance for signal (determined from ISAJET Monte Carlo with $m_t = 180$ GeV), $\mathcal{L}$ is the integrated luminosity, and the cross section, $\sigma_{t\bar{t}}$, is to be determined from the fit.

We then fit for $\sigma_{t\bar{t}}$ and ϵ, taking the uncertainty in each N_i to be $\sqrt{N_i}$. MINUIT [14] is used to minimize the χ^2. The fit returns $\sigma_{t\bar{t}} = 4.0 \pm 4.8$ pb and $\epsilon = 0.034 \pm 0.005$, with $\chi^2/\mathrm{DOF} = 6.2/4$. We note that the fitted value of ϵ is in good agreement with the average tagging rate derived from Equation 1, and that $\sigma_{t\bar{t}}$ agrees with the value obtained in Section 5.

Using the results of the fit and Eqs. 2 and 3, we can determine the number of background events in each of the six event samples. The results are shown in Table 4, where in each case, we have added the events in sets A_i through A_6. The full error matrix has been used to determine the uncertainties on these sums. The maximum statistical significance is expected to be achieved using the criteria of Set 6. For these criteria, the $t\bar{t}$ cross section corresponding to the observed excess (4 events) is 4.4 ± 4.9 pb, which agrees well with the result of the fit. It also agrees with the results of the analysis using the grid search (see Section 5).

Furthermore, we can use the muon-tagging rate (ϵ) to determine the expected background for doubly muon-tagged events. The probability that an event has two muon-tags is $\epsilon^2 e^{-\epsilon}/2!$. Using the kinematic criteria of Table 3 leads to the results shown in Table 5. (Again, all errors have been propagated using the full error matrix.) For the criteria that yield maximum expected statistical significance (*i.e.*, Set 3), we find an excess of 0.59 event, corresponding to a $t\bar{t}$ cross section of 3.9 ± 9.8 pb.

Set No.	data	N($t\bar{t}$+bkg) fit	N(bkg) fit	excess (data−bkg)	N($t\bar{t}$) fit
1	142	135.96	124.77 ± 19.15	17.23 ± 22.56	11.20
2	111	105.55	95.41 ± 14.95	15.59 ± 18.29	10.14
3	97	91.36	81.81 ± 12.98	15.19 ± 16.30	9.56
4	80	69.39	60.91 ± 10.12	19.09 ± 13.51	8.48
5	37	39.73	33.23 ± 5.87	3.77 ± 8.45	6.50
6	15	14.68	10.99 ± 2.33	4.01 ± 4.52	3.69

Table 4: Results of the search for $t\bar{t} \to$ all-jets. For each set of kinematic critera from Table 3, the number of background and $t\bar{t}$ events has been determined from the results of the χ^2 fit.

Set No.	data	N(bkg) from fit	excess	N($t\bar{t}$) from fit
1	2	2.15 ± 0.64	-0.15	0.71
2	2	1.64 ± 0.50	0.36	0.64
3	2	1.41 ± 0.43	0.59	0.61
4	1	1.05 ± 0.32	-0.05	0.54
5	1	0.57 ± 0.18	0.43	0.41
6	0	0.19 ± 0.07	-0.19	0.23

Table 5: Results for doubly muon-tagged events, using the six sets of kinematic criteria from Table 3.

7 Outstanding Issues

7.1 Corrections to the Jet Energy Scale

We have observed that the jet-energy scale corrections of CAFIX are not sufficient for matching jet energies to the parton energies. In the kind of measurement/search that we have described, matching the energy scales of reconstructed jets in data and Monte Carlo is more important than matching jet energies to parton energies, but we have nevertheless devoted some effort to improving the CAFIX corrections. Among the effects we have studied are:

- The momentum of the muon should be added to tagged jets. We have studied additional corrections to account for the lost momentum of the neutrino and for the effect of momentum resolution in the muon chambers.
- A small correction for energy lost due to radiation outside the jet cone should be applied.
- Version 5.0 of CAFIX includes a correction for for the effect of luminosity; however, the size of the necessary correction appears to be underestimated. We are presently studying the effect in order to make additonal corrections.

We have not yet included any of these corrections in our analysis. They will be discussed in detail in a forthcoming DØ Note.

7.2 Mass Measurement

Extracting the mass of the top quark in the all-jets channel is extremely difficult due to the weak signal. The problem is further complicated because our kinematic criteria, especially the requirements on H_T^{3j} and N_{jets}^A, introduce a bias toward events with large reconstructed mass. Consequently, only small differences exist between the mass distributions for signal and for background. In order to measure the mass of the top quark from our data, we must improve the significance of the signal and reduce the mass bias in the selection criteria.

In the meantime, the mass analysis may provide additional discrimination for the measurement of the $t\bar{t}$ cross section. For instance, every $t\bar{t} \rightarrow$ all-jets event contains two W bosons that decay hadronically. If these particles can be reconstructed, we may achieve additional power to discriminate against background. This possibility has not as yet been fully explored.

8 Summary and Conclusion

We have searched for $t\bar{t}$ production in the all-jets channel. Using an integrated luminosity of 79.6 pb^{-1}, we find 15 events in the singly muon-tagged channel, with an expected background of 10.99 ± 2.33 events. In the doubly muon-tagged channel, we find 2 events with an expected background of 1.41 ± 0.43 events. These results correspond to cross sections for $t\bar{t}$ production of 4.4 ± 4.9 pb and 3.9 ± 9.8 pb, respectively. Although we do not observe a significant signal, we hope to improve our sensitivity by further refining the analysis, and in particular, by gaining a better understanding of the muon-tagging rate for background.

Acknowledgements

We thank Marc Paterno for the alternative calculation of the $t\bar{t}$ cross section that appears in the Appendix. We thank the members of the top group for helpful discussions, and Tom Ferbel for detailed editorial comments.

References

[1] C. Stewart, C. Cretsinger, "Preliminary Study of Parameters for Top to Jets Event Selection," DØ Note 2499, 1995

[2] C. Cretsinger, for the DØ Collaboration, *Search for Top in the All-jets Channel at DØ*, Bull. Am. Phys. Soc. (1995).

[3] C. Stewart, C. Cretsinger, E. Won, "Search for the Top Quark in the All-jets Channel at DØ," DØ Note 2588A, 1995

[4] C. E. Cretsinger, *Search for the Top Quark in the All-Jets Channel*, Ph.D. Thesis, University of Rochester, 1995. (Available as DØ Note 2825.)

[5] G. Manning *et al.* (DØ Collaboration), "DØ Software Documentation" (in preparation), July 1995.
URL: `http://d0wop.fnal.gov/software/offline_document.ps`

[6] T. Joffe-Minor, R. Astur, "A Study of the Effects of the CAFIX Energy Scale Corrections," DØ Note 2211, 1994 (unpublished).

[7] M. Narain, J. Hobbs, private commnunication.

[8] J. Hobbs, H. Zhu, private communication.

[9] S. Ahn *et al.*, "Another Look at *b*-quark Tagging with Soft Muons," DØ Note (in preparation).

[10] N. Amos *et al.*, "The Random Grid Search: A Simple Way to Find Optimal Cuts" (Talk given at the 1995 Computing in High Energy Phsyics Conference, Rio de Janeiro, Brazil), DØ Note 2791, 1996.

[11] J. Moromisato, "The DVF Method," DØ Note (in preparation).

[12] C. Petersen, T. Rognvaldsson, *Comp. Phys. Comm.* 81:185–200, 1994.

[13] P. C. Bhat, "Search for the Top Quark at DØ Using Multivariate Methods," FERMILAB-Conf-95/211-E.

[14] M. Goosens *et al.*, *MINUIT*, CERN Program Library Number D506 (1992).

[15] I. Bertram *et al.*, "A Recipe for the Construction of Confidence Limits," DØ Note 2775A (1995).

Appendix: Alternative Calculation of $\sigma_{t\bar{t}}$

Here, we follow the procedure described in DØ Note 2775 [15] to calculate the probability density functions for the $t\bar{t}$ cross section, determined from the results reported in Section 6 for the doubly-tagged and singly-tagged channels.

Given the observed event yield, the calculation uses Bayes' Theorem to determine the posterior probability distribution for $\sigma_{t\bar{t}}$, assuming a uniform prior probability density for the cross section, *i.e.*,

$$P(\sigma) = \begin{cases} 1/\sigma_{max} & 0 < \sigma < \sigma_{max} \\ 0 & \text{otherwise} \end{cases} \tag{5}$$

Details of the calculation are given in Ref. [15].

For the doubly-tagged channel, we use the criteria of Set 3, for which we observed 2 events with an expected background of 1.41 ± 0.43 events, corresponding to an integrated luminosity of 70.3 ± 3.5 pb^{-1}. The acceptance for $t\bar{t}$ is determined from Monte Carlo to be 0.00215 ± 0.00040. The results of the calculation are shown in Fig. 10. We see that the peak of the probability density function corresponds to a cross section of 4.4 pb, and that the function has a long tail corresponding to large possible cross sections. Fig. 11 represents the probability that $\sigma_{t\bar{t}}$ is less than the value of the abscissa. We see that this function asymptotically approaches unity, which indicates that our chosen value of σ_{max} (80 pb) was large enough that it does not affect the calculation.

Because the probability density function is highly asymmetric, the mean value of σ is not a reliable estimator of $\sigma_{t\bar{t}}$. We choose instead the most probable value, with an uncertainty determined by the smallest 68.3% confidence interval around that value. Using this choice, we find $\sigma_{t\bar{t}} = 4.4^{+13.1}_{-4.4}$ pb.

For the singly-tagged channel, we use the criteria of Set 6, for which we observed 15 events with an expected background of 10.99 ± 2.33. The acceptance for $t\bar{t}$ for these criteria is 0.01308 ± 0.00328. Again, using the most probable value and the smallest 68.3% confidence interval around that value, we find $\sigma_{t\bar{t}} = 4.3^{+5.1}_{-4.3}$ pb. Both the singly-tagged and doubly-tagged results are consistent with those of Section 6, but have the advantage that unphysical values ($\sigma_{t\bar{t}} < 0$) are excluded.

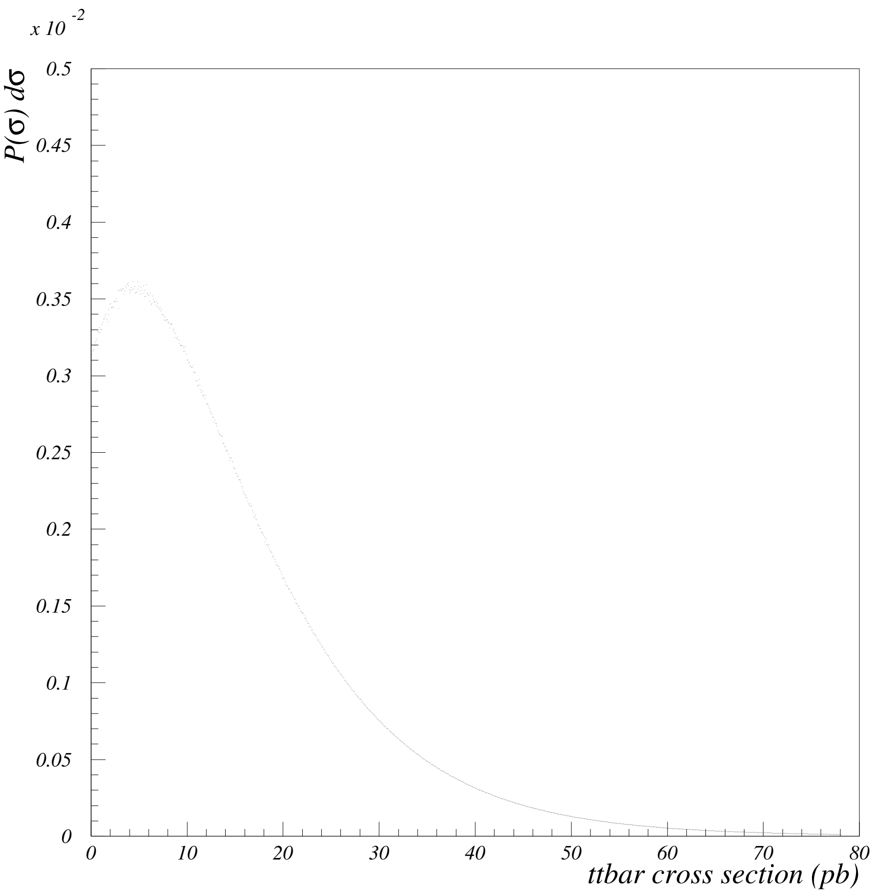

Figure 10: Posterior probability density function for $\sigma_{t\bar{t}}$, based on the double-tagged $t\bar{t} \rightarrow$ all-jets channel.

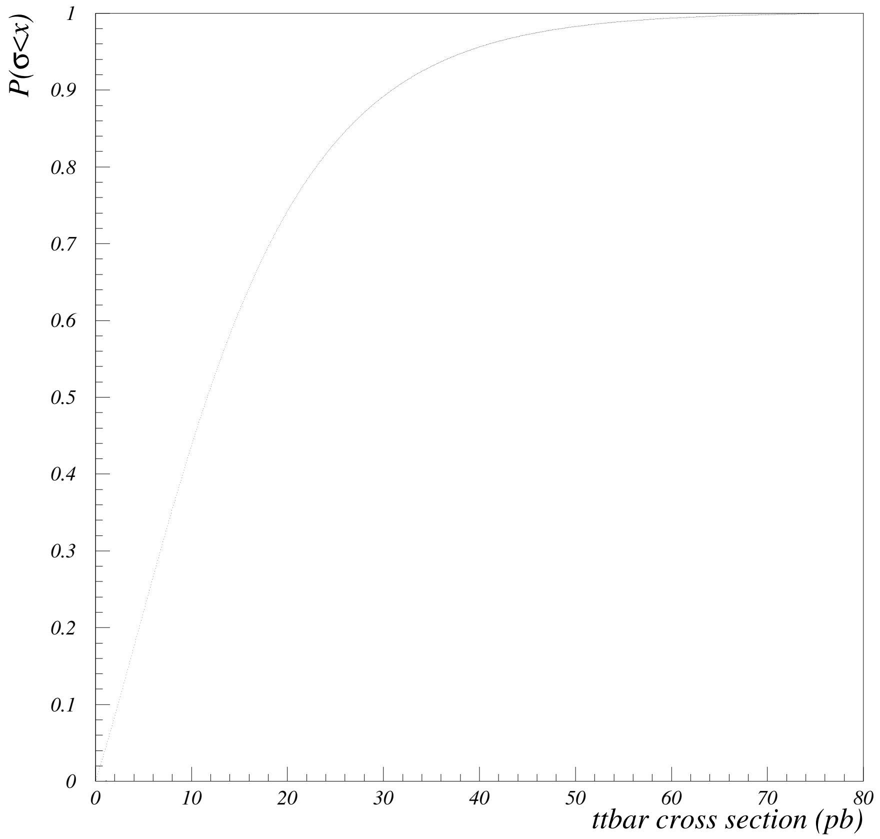

Figure 11: Probability that $\sigma_{t\bar{t}}$ is less than the value of the abscissa.